Collaboratively Harvesting Ambient Radiofrequency and Thermal Energy

Lei Guo, Xiaoqiang Gu, Peng Chu, Simon Hemour, Ke Wu

Collaboratively Harvesting Ambient Radiofrequency and Thermal Energy

Lei Guo, Xiaoqiang Gu, *Student Member, IEEE,* Peng Chu, *Member, IEEE,* Simon Hemour, *Senior Member, IEEE, and* Ke Wu, *Fellow, IEEE*

***Abstract*—In this paper, an ambient power harvester with a single diode device is proposed for simultaneously scavenging both radiofrequency (RF) and thermal energy in a mixed and cooperative manner. This cooperative harvesting process is theoretically examined through a proposed model of diode and then validated by simulation and measurement. In the proposed cooperative power harvester, the harvested dc voltage from thermal source is used to bias the diode for improving the diode's RF-to-dc power conversion efficiency (PCE). An accurate analytical model of Schottky diode is developed for specifying the constraining parameters of RF-to-dc PCE and accurately predicting diode's performances in a low RF power range (≤–25 dBm), respectively. The calculated results are found to be in a good agreement with the simulated ones obtained by the harmonic balance simulator in Advanced Design System (ADS). For demonstration and validation, the proposed mixed cooperative power harvester is designed and prototyped on the basis of diode SMS7630. A total measured output dc power around 0.8 μW is obtained with an RF-to-dc PCE around 33.4%, when the two injecting power sources at the diode are both –30 dBm. In addition, rectennas with and without a matching network are both fabricated and tested. By eliminating the L matching network, the rectenna is found to offer a higher dc output power. The proposed mixed cooperative power harvester is hoped to find potential real-world applications in ambient atmosphere with RF coverage and temperature gradient. It not only helps to produce a higher power but also provides a reliable way of improving the resilience of dc power production.**

***Index Terms*—Analytical model, cooperative ambient power harvester, low-power scavenging, radiofrequency (RF) energy, RF-to-dc power conversion efficiency, and thermal energy.**

Manuscript received Oct. 24, 2018; accepted Apr. 6, 2019. This work is supported under the grant DUT19RC(3)014 at Dalian University of Technology and in part by the Natural Sciences and Engineering Research Council (NSERC) of Canada.

L. Guo is now with the School of Information and Communication Engineering, Dalian University of Technology, Dalian, China. She was with the Poly-GRAMES research center, École Polytechnique de Montréal, Montreal, QC H3T 1J4, Canada (e-mail: leiguo@dlut.edu.cn).

X. Q. Gu and K. Wu are with the Poly-GRAMES research center, École Polytechnique de Montréal, Montreal, QC H3T 1J4, Canada.

P. Chu is with the College of Electronic and Optical Engineering, Nanjing University of Posts and Telecommunications, Nanjing 210023, China. (Corresponding author: realchu@gmail.com)

S. Hemour is with CNRS and the IMS research center, Dept. of Science and Technology, University of Bordeaux, France.

I. Introduction

AMBIENT energy scavenging has attracted significant attention for self-powered micro-systems and/or wireless sensor nodes in the realization of a smart environment [1]. The widely utilized ambient energy sources are electromagnetics, vibration (kinetic), thermal, motion, wind, solar and so on [2-5]. As one of the multiple sources, wireless radiofrequency (RF) energy has been extensively investigated in the context of energy harvesting because of its pervasiveness such as TV, radio, cellular, satellite, and Wi-Fi signals. It is shown that the ambient RF power density is usually less than 1 $\mu W/cm^2$. Because of its limited power density, harvesters scavenging ambient RF energy generally suffer from low power conversion efficiency (PCE). For example, it has been demonstrated that the PCE of a single diode based harvester is normally less than 10% if the input power level is lower than –30 dBm [6]. To leverage the PCE, diodes with stronger nonlinearity have been employed such as spindiodes [6], backward tunneling diodes [7] and nanodiodes [8]. However, these diodes require extremely challenging fabrication processes due to the constraints of physical principles and accessible materials. An alternative approach is to increase the available source power. Some hybrid or mixed power harvesters have been proposed by integrating several power sources together [9-15]. Among these demonstrations, a power harvesting scenario is incorporating RF power (AC power) and converted dc power (solar/thermal source) [9, 13, 14]. A hybrid power harvester incorporating a solar cell and rectenna was proposed in [9]. As the RF and solar energy are harvested separately, the RF-to-dc PCE is only around 15% when the RF power level is –20 dBm. In [13], a highly integrated power harvester was developed to harvest energy sources of solar, artificial light, thermal, and RF. It focuses on the design topology to achieve high circuitry integration and output power. Recently, a thermal source is used as the diode's bias for cooperative energy scavenging in a mixed harvester [14]. Although some losses are introduced using the generated dc voltage as a bias, the bias can shift the diode operating point, leading to a much higher RF-to-dc PCE. The work is valuable from the standpoint of economical relevance that is defined as the ratio of output value to input cost. This is because thermal gradient (thermal sources) can be found in many places and can be considered as a free source, while RF sources can be costly due to its obtainment from the ad-hoc sources. However, no analytical method was given to theoretically estimate the

diode's output and explicitly indicate key controlling parameters.

In this paper, a mixed cooperative ambient RF and thermal power harvester is proposed and rigorously analyzed. By utilizing the dc voltage converted by a Thermoelectric Generator (TEG) to bias the diode, the RF-to-dc PCE can be enhanced in the ambient power range (<−25 dBm). An accurate analytical model is developed for both qualitative and quantitative analysis. Using the model, the key parameters controlling RF-to-dc PCE can clearly be revealed. On the other hand, the model is capable of predicting the diode's output power and RF-to-dc PCE in a more realistic scenario. It is used for the evaluation of a typical Schottky diode SMS7630, which is validated by simulation using a harmonic balance simulator in Advanced Design System (ADS). For demonstration, the mixed cooperative power harvester is designed and fabricated with measured results reasonably agreeing with simulated and calculated ones, further verifying the proposed analytical model. Besides, the rectenna of such a mixed cooperative power harvester is designed without a matching network and measured under different RF source illustrating conditions. It can output a higher dc power than the rectenna with *L* matching network.

The paper is arranged as follows: Section II gives the diode's analytical model and the evaluation of diode SMS7630 using the proposed model. A mixed cooperative power harvester based on diode SMS7630 is demonstrated in Section III for validation. Section IV shows the rectenna design, measurement setup, and measured results. Section V concludes the contribution of the work.

II. Theoretical Analysis

A. Accurate Model

Figure 1 (a) shows the schematic diagram of a single-diode based mixed cooperative RF and thermal power harvester. The thermal power is harvested through a TEG device based on Seebeck effect [16] which is capable of generating dc voltage using a temperature gradient between two dissimilar conductors or semiconductors. The RF and thermal sources are assumed to have internal or equivalent internal resistors of R_{01} and R_{02}, respectively. It should be mentioned that the TEG with small resistance R_{02} is selected in the design to provide a dc bias close to the voltage converted by the TEG source. For isolation between the two source ports, dc block C_1 and RF choke L_2 are deployed. For a typically packaged diode, the packaging effect is usually modeled as parasitic inductor L_p and capacitor C_p. At the load, capacitor C_L is placed in parallel with load resistor R_L to smooth out AC component. The Shockley model is utilized for the diode analysis as shown in Fig.1(b) which includes a nonlinear junction resistor R_j, junction capacitor C_j and series resistor R_s.

The RF source is assumed as a sinusoidal wave signal with a voltage of $V_{RF} = v_1\, cos(2\pi f_1 t)$. Here, v_1 and f_1 are the voltage magnitude and source frequency, respectively. It should be mentioned that only the fundamental component of the RF source is considered to reach the diode, as the higher-order harmonics could be filtered out by designing a

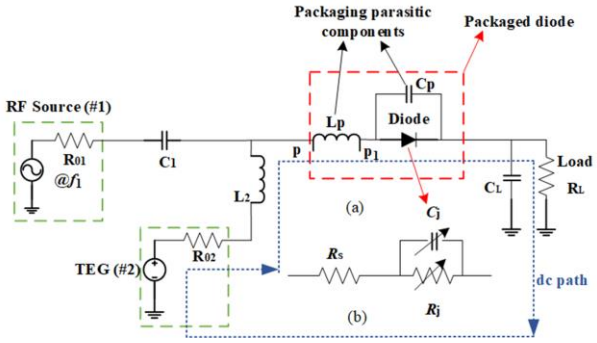

Fig. 1. (a) Schematic diagram of single-diode based mixed cooperative RF and thermal power harvester. (b) Shockley model of the diode.

proper matching network [17]. The dc voltage converted by TEG and the total rectified voltage across R_L are defined as v_{TEG} and v_l, respectively. Thus, the voltage across the nonlinear junction resistor R_j is defined as V_{in} which can be calculated as:

$$V_{in} = V_{RF} + v_{TEG} - v_l \tag{1}$$

The load voltage v_l is easily obtained by multiplying dc current i_l by total resistance R_t in the dc path. As the dc current i_l cannot go through the RF source due to the dc block capacitor C_1, R_t is obtained as $R_L + R_s + R_{02}$.

Using the Shockley model, the exponential *I-V* relationship of the Schottky diode can be written as:

$$I_d = I_s \cdot \left[e^{\frac{V_{in}}{n \cdot V_t}} - 1 \right] \tag{2}$$

where I_s and n are saturation current and ideality factor of the diode which may vary with different diodes. The parameter of V_t is the thermal voltage which is defined as $V_t = k \cdot T/q$ with k, T ,and q representing the Boltzmann constant, operating temperature and electron charge, respectively. The value of V_t is usually constant when the temperature T is fixed. It should be mentioned that the exponential model (2) can be considered accurate within this low-power range.

To obtain different harmonic components of the current, a method of Taylor expansion has been utilized but showing some truncation errors [10]. This problem can be solved by expanding the exponential term with the Bessel function, shown as:

$$e^{\frac{V_{RF}}{n \cdot V_t}} = J_0\left(-i\frac{v_1}{n \cdot V_t}\right) + 2\sum_{k=1}^{\infty} g(k)\, cos[k \cdot (2\pi f_1 t)] \tag{3}$$

where g(k)= $i^k J_k\left(-i\frac{v_1}{n \cdot V_t}\right)$, in which $J_k(x)$ is the Bessel function of the first kind of order k. After extracting the dc component in (3) and substituting the extracted term in (2), the solution of i_l can be obtained as:

$$i_l = I_s \cdot \left(\frac{W_0(x)}{G} - 1\right) \tag{4}$$

where $W_0(x)$ is the 0th branch of the Lambert-W function with x given by $G \cdot J_0\left(-i\frac{v_1}{n \cdot V_t}\right) \cdot e^{\frac{v_{TEG}}{n \cdot V_t}} \cdot e^G$. The parameter G is defined as $(R_L + R_s + R_{02})/R_{j0}$, in which $R_{j0} = n \cdot V_t/I_s$ is the zero bias junction resistance of the diode. As R_{02} is very small compared to R_{j0}, it shows negligible effects on i_l in (4). After obtaining i_l in (4), the output dc power P_l at load R_L can be easily calculated by:

$$P_l = i_l^2 \cdot R_L \quad (5)$$

The injected dc power from TEG and RF power can be written as:

$$P_{TEG} = i_l \cdot v_{TEG}. \quad (6)$$

$$P_{\mathrm{RF}} = real\left(\frac{V_{\mathrm{p}} \cdot I_p^*}{2}\right) \quad (7)$$

where $V_{\mathrm{p}}$and I_{p} are the voltage and current of RF source at node p in Fig.1(a). To obtain the values of these two parameters, the voltage $V_{p_1}$and current $I_{p_1}$of RF source at p_1 are calculated first as:

$$V_{p_1} = V_{RF} + \left(I_1 + V_{RF} \cdot i\omega C_j\right) \cdot R_s \quad (8)$$

$$I_{p_1} = I_1 + V_{RF} \cdot i\omega C_j \quad (9)$$

where $\omega = 2\pi f_1$is the angular frequency of RF source. The parameter I_1 is the fundamental RF current going through R_{j}. It can be obtained using (2) and (3), which can be written as:

$$I_1 = I_s \cdot \left[2 \cdot i \cdot J_1\left(-i\frac{v_1}{n \cdot V_t}\right) \cdot e^{\frac{v_{TEG}-v_l}{n \cdot V_t}}\right] \cdot cos(2\pi f_1 t) \quad (10)$$

It should be noted that I_1 is assumed to be in-phase with V_1 in the calculation. Using V_{p_1} and I_{p_1}, parameters V_{p} and I_{p} can be easily calculated at the packaged diode (Fig.1 (a)):

$$I_p = V_{p_1} \cdot i\omega C_p + I_{p_1} \quad (11)$$

$$V_{\mathrm{p}} = V_{p_1} + I_{p_1} \cdot i\omega L_p \quad (12)$$

By substituting (10) into (11) and (12), the injecting RF power in (7) can be therefore obtained. It should be noted that we only consider how the power is converted in the diode when the source power reaches the diode. Only parasitic components of the diode are considered because they have impact on the power converted in the diode. For C_1 and L_2, they will not interact with the nonlinear conversion of the diode. As a result, the parasitics of C_1 and L_2 are neglected here for simplicity without affecting the proposed model. Using the accurate model formula, the output dc power P_{l} can be easily obtained if both source power levels are given [18].

The RF-to-dc PCE η_{RF-dc} and total PCE η can be calculated as:

$$\eta_{RF-dc} = \frac{P_l - P_{l\_TEG}}{P_{RF}} \times 100\% \quad (13)$$

$$\eta = \frac{P_l}{P_{RF} + P_{TEG}} \times 100\% \quad (14)$$

where $P_{l_TEG}$is the output power at load in the mixed power harvesting scenario without RF source input. Using (13), η_{RF-dc} can be further written as

$$\eta_{RF-dc} = \frac{R_j^{\,2}\Re_{I0}}{R_L + R_s + R_j} \cdot \left(\Re_{I0} P_{RF} + 2i_{l\_TEG}\right) \quad (15)$$

where $\Re_{I0}$is the short circuit current responsivity defined as the ratio of rectified RF-to-dc current to input RF power P_{RF}, at short circuit condition, while $i_{\mathrm{l\_TEG}}$ is the dc current contributed by the thermal source. It can be observed from (15) that $\eta_{RF-dc}$is a function of R_j, R_L, $\Re_{I0}$, P_{RF}, and i_{l_TEG}. When the other parameters are fixed, the higher RF source power P_{RF} will result in the higher the RF-to-dc PCE. The result is consistent with that in a zero-bias scenario [6]. Also, the efficiency is directly related to i_{l_TEG} which is a parameter direct proportional to the applied v_{TEG}. Another important parameter $\Re_{I0}$ is limited by the fabrication technology and has a maximum value of 19.34 A/W for Schottky diode at room temperature of 300K [19]. In order to maximize (15), a Schottky diode with higher R_j and lower R_s is preferable.

According to (15), η_{RF-dc} can be qualitatively analyzed. The formula would be useful as a rough guideline for selecting a desirable diode when designing such a mixed cooperative power harvester. However, in a realistic scenario, these key parameters are related to each other. The proposed formula (1)-(12) can give a more realistic quantitative analysis of the diode making a comprehensive evaluation, which will be shown in part B.

B. Evaluation of SMS7630 using Accurate Model

The mixed cooperative power harvester based on typical diode SMS7630-079LF is calculated in this part for evaluation. The SPICE and packaging parameters of the diode are given in Table I. Using the accurate model, the current responsivity $\Re_I\left(i_l\right)$ considering the load condition is rewritten as:

$$\Re_I\left(i_l\right) = \frac{i_l - i_{l\_TEG}}{P_{RF}} = f(v_1, v_{TEG}, \frac{R_L}{R_{j0}}) \quad (16)$$

After substituting (4) into (16), it can be found that $\Re_I\left(i_l\right)$ is a function of v_1, v_{TEG}, and $\frac{R_L}{R_{j0}}$. For a given 2.4 GHz RF source with a power level of –40 dBm, the calculated $\Re_I\left(i_l\right)$ contour as a function of v_{TEG} and $\frac{R_L}{R_{j0}}$ for SMS7630 is shown in Fig. 2. With reference to Fig.2, a lower R_{L} can lead to a higher $\Re_I\left(i_l\right)$.

TABLE I
SPICE AND PACKAGING PARAMETERS OF SMS7630-079LF

Parameters	I_s	n	R_s	C_{j0}	L_p	C_p
Units	A	/	Ω	pF	nH	pF
Value	5e-6	1.05	20	0.14	0.7	0.16

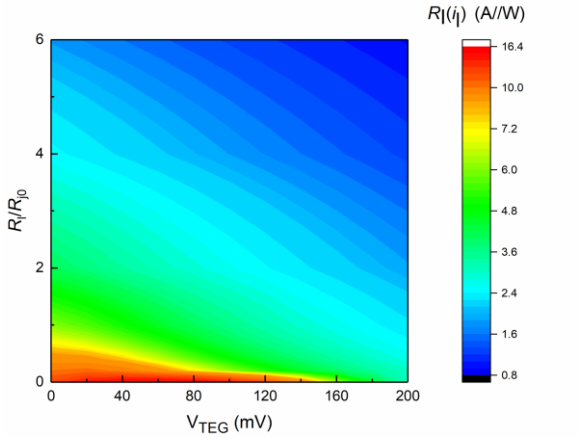

Fig. 2. Calculated $\Re_I\left(i_l\right)$ using accurate model for P_{RF}=–40 dBm with v_{TEG} and $\frac{R_L}{R_{j0}}$ changing from 0-200mV and 0-6, respectively. The calculation is based on SMS7630.

When $\frac{R_L}{R_{j0}}$ is relatively small (< 0.3), $\Re_I\left(i_l\right)$ may increase at small v_{TEG} but decrease with larger v_{TEG}.

Referring to (14), η_{RF-dc} is also associated with $R_j\left(i_l\right)$, and i_{l_TEG}except $\Re_I\left(i_l\right)$. To investigate the effects of v_{TEG} on these four parameters ($R_j\left(i_l\right)$ $\Re_I\left(i_l\right)$, η_{RF-dc} and i_{l_TEG}), Fig. 3 shows the calculated trend of each parameter for a fixed RF power of −30 and −40 dBm. For the ease of calculation, R_L is fixed and equal to R_{j0}. The voltage range 0-200mV is selected as it is enough for the ambient power level <−25 dBm. With reference to Fig.3(a), both $R_j\left(i_l\right)$ and $\Re_I\left(i_l\right)$have the same tendency which declines as v_{TEG} is enlarged. However, because of the increased bias current i_{l_TEG}, η_{RF-dc} is enhanced as a result as shown in Fig3.(b). It should also be noted that although a higher η_{RF-dc} is achieved with a larger v_{TEG}, the enhancement of η_{RF-dc} reduces gradually. For the validation of calculated results, the mixed cooperative power harvester is also simulated in ADS with the simulated η_{RF-dc} compared in Fig.3. A reasonable consistency can be observed between the calculated and simulated results, thus verifying the accuracy of the model. Fig. 4 shows the calculated and simulated total PCE with a good agreement between each other.

The above calculation has theoretically pointed out the key controlling parameters that affect the RF-to-dc PCE of such a

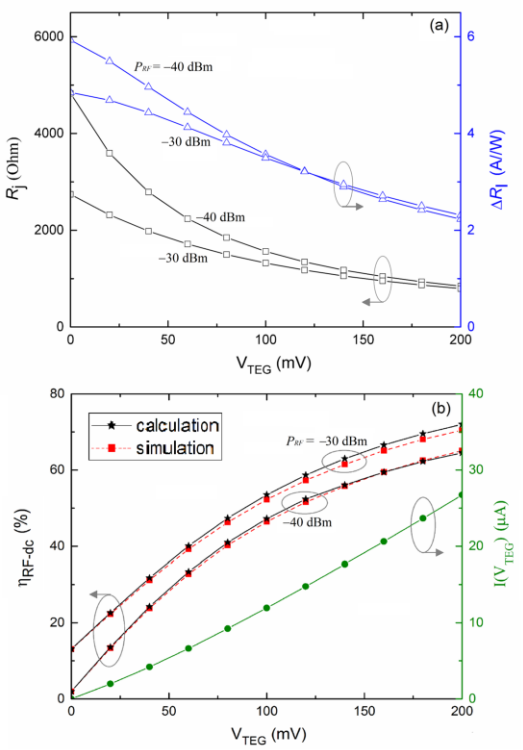

Fig. 3. When v_{TEG} is changed from 0 to 200mV, calculated $R_j(i_l)$, $\Re_I\left(i_l\right)$, η_{RF-dc}, and i_{l_TEG} are plotted for P_{RF} = −30 dBm and −40 dBm. (a) Calculated $R_j(i_l)$ and $\Re_I\left(i_l\right)$ (b) Calculated η_{RF-dc} and i_{l_TEG}. The simulated η_{RF-dc} is compared for validation. The calculation and simulation is based on diode SMS7630.

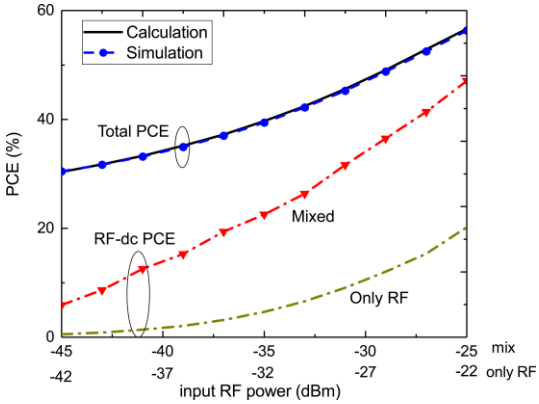

Fig. 4. Calculated and simulated total PCEs of the proposed mixed cooperative power harvester. Measured RF-dc PCEs of the proposed mixed cooperative and single RF power harvesters. Calculation and simulation are based on diode SMS7630.

mixed cooperative power harvester topology. It can be found that the formula can accurately predict the RF-to-dc PCE and total PCE in each power level, which helps to clearly show the benefits of the mixed power harvester. Besides, the required TEG and RF voltages in the mixed power harvesting can be also accurately estimated using the proposed formula for given power levels.

III. Measurement and Model Validation

The experimental prototype of the proposed mixed cooperative power harvester is designed and fabricated on a substrate material of Rogers RT/Duroid 6002 which has a dielectric constant of 2.94 and thickness of 20 mils, as shown in Fig. 5. The RF source frequency is 2.4 GHz. A typical L matching network is employed to match the RF source to the diode. To harvest the thermal source, a Peltier device with the part number of CP60240 is used. The load resistor (R_L) is 5.6 kΩ. It should be mentioned that as our demonstration is used for validating the proposed analytical model, R_L is kept the same as R_{j0} considering the power range of interest is at ambient level (<−30 dBm). The components C_1 and L_2 with high Q factors from Johanson Technology Inc. are selected with part numbers of 201R07S270JV4S and L-07C27N#V6T, respectively.

Figure 6(a) displays the measurement setup of the mixed cooperative power harvester. An external signal generator is used to provide the RF source. Two multimeters are employed to measure the dc voltages converted by TEG and output rectified by diode at R_L, respectively. The thermal measurement

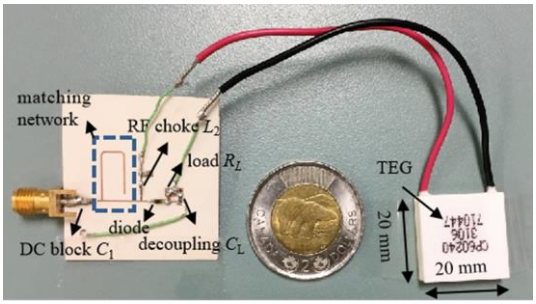

Fig. 5. The prototype of the proposed mixed cooperative power harvester.

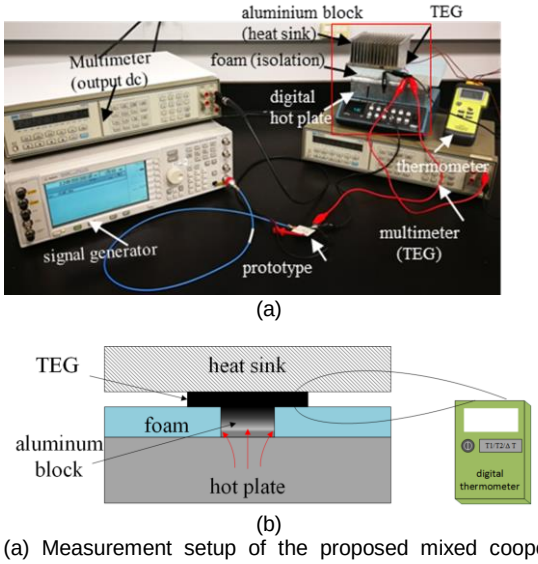

Fig.6. (a) Measurement setup of the proposed mixed cooperative power harvester. (b) Diagram showing the thermal source setup.

setup is used for demonstration which can be avoided in practical applications. In the setup, the hot side of TEG is heated for generating the temperature difference with the cold side (ambient temperature). The temperature difference can be monitored by a thermometer. Using the temperature gradient, the TEG can produce dc voltage v_{TEG} working as the bias which can be monitored using the previously mentioned multimeter. For the thermal source setup, a thick foam is used as the heat isolator with a rectangular hole reserved for a small aluminum block serving as the heating source. The TEG is placed on the top of the small aluminum block. To better control the temperature variance of TEG, a bulky aluminum block is introduced and placed on the TEG as the heat sink. The bulky aluminum block can simultaneously ensure a good contact between the TEG and the small aluminum block (heating source). A detailed illustration of the thermal source setup is given in Fig.6 (b). Such a measurement setup is used for better controlling the temperature difference, thus the required dc voltages for different power levels. As shown in Fig. 6(a), the measured dc voltage converted by TEG and temperature difference across the two sides of TEG can be collected at the same time.

In both simulation and measurement, the power from TEG and RF source reaching the diode are kept the same and swept from −45 to −30 dBm. The power from TEG means the dc power reaching the diode, which can be calculated using (6). For providing the required power level, the corresponding TEG voltage v_{TEG} can be calculated preliminarily using the proposed analytical model. In the measurement, we just need to monitor the TEG voltage v_{TEG} caused by the temperature gradient. Figure 7(a) shows the calculated, simulated, and measured output dc power of the mixed cooperative power harvester against the injected source power level. For the mixed cooperative power harvester, the two source power levels are kept the same. The required temperature gradient is given in the upper axis of Fig.7(a), which corresponds to the power level shown in the lower axis. It should be noted that a high temperature gradient is needed across the two sides of TEG in

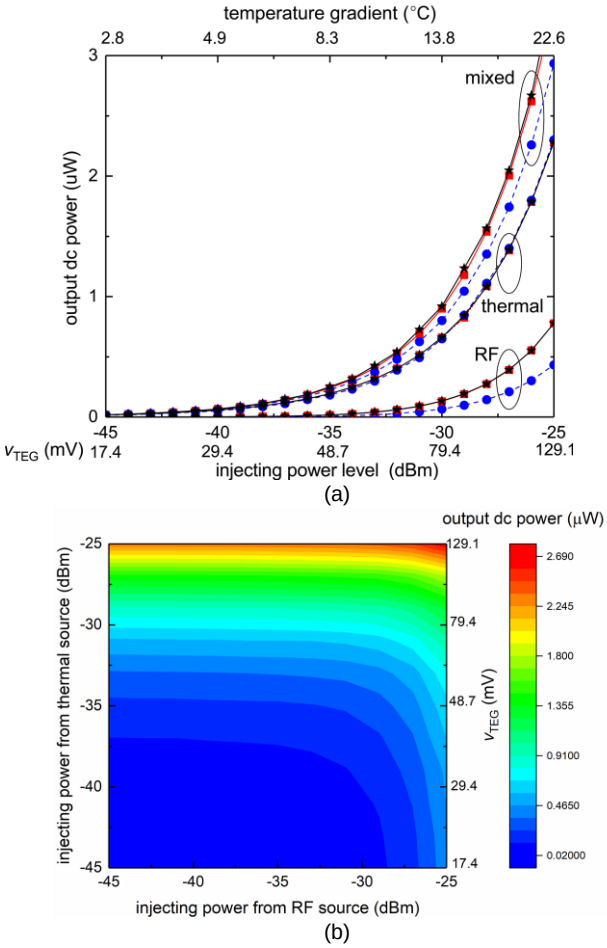

Fig. 7. (a) Calculated, simulated, and measured output dc power of the proposed mixed cooperative power harvester with RF and thermal sources, with thermal source, and with RF source input. The RF and thermal power are kept the same.(b) Measured output dc power of the proposed mixed cooperative power harvester with RF and thermal source varying from −45 dBm to −25 dBm. v_{TEG} corresponds to the bias voltage when the two source power are equal.

order to obtain enough biasing dc voltage on the diode. It is because the diode's junction resistance R_{j0} is much larger than the TEG's internal resistance R_{02}, leading to a low power transfer efficiency from the TEG to the diode. Again, a reasonable consistency is obtained between the calculated and simulated results, thereby validating the proposed analytical model. The measured result is observed slightly lower than the calculated and simulated counterparts. This discrepancy should be caused by the unaccounted losses of lumped components and imperfection of the experiments. For comparison, the output dc power of each single source input scenario is also plotted in Fig.7(a). A reasonable agreement is also observed between results in calculation and simulation for each case, thus showing that the analytical model also applicable for single source input scenario. Besides, the mixed cooperative power harvester can be found to produce higher power than the scenario with a single RF/thermal input. Although the thermal power harvesting is the dominant contributor to the power range of interest, the contribution of RF power harvesting becomes more significant with the increase of RF power. It is reasonable that the RF PCE increases dramatically with a larger injecting power. Moreover, it is also found that the RF-to-dc

power can be significantly enhanced in a very low power level (~9.4 times @−45dBm in the calculation) when keeping the two source power same. But the enhancement decreases with a higher injecting power (~1.68 times @−25dBm in the calculation). Figure 7(b) shows the measured output dc power of the mixed cooperative power harvester, when each of the sources is varied from −45 dBm to −25dBm.

To show the advantage of the proposed mixed cooperative power harvester, the measured RF-to-dc PCE is compared with the single RF power harvester with result shown in Fig.4. To ensure a fair comparison, the total input power levels in the two cases are kept the same. As expected, a significant improvement in RF-to-dc PCE can be observed. It clearly demonstrates the merits of the proposed mixed harvester in RF-to-dc PCE, making it useful for practical application scenarios considering the economical relevance [14].

The cooperative interaction between the two sources can be found in two aspects. One of the aspects is a significant improvement in RF-to-dc PCE (evidenced in Fig.4). For the other, the input source voltages were found lower in the mixed power harvesting than those in the single source cases, if the same amount of power reaches the diode.

IV. Rectenna Design

Different from the ideal RF input provided by a single generator in Section III, we designed an antenna to integrate it with the harvester forming a rectenna in order to make it capable of scavenging the ambient RF power. The rectenna in this part is proposed for demonstrating the mixed RF-TEG power harvesting in a more realistic way. As the previous model only considers the power reaching the diode, the antenna design will not affect the previous analysis. But the parameters of return loss and antenna gain will determine the received power, and thus the final output power, when the ambient power density is fixed. To verify the previous analysis directly, the matching network is excluded by matching the antenna to the diode input. It means that the rectenna is expected to show the similar output power when the antenna receives the same amount RF power as in Section III. In such a way, the rectenna demonstrates a realistic realization of the mixed RF-TEG harvester.

In this part, the antenna design is firstly given including the key parameters of return loss, antenna gain and radiation patterns. Then, it is investigated to use the designed antenna to scavenge the RF power in a mimetic RF environment. Finally, the rectenna is tested with the RF and thermal power input.

A. ANTENNA

Bowtie slot antenna is employed here because of its wideband impedance bandwidth which can make the entire harvester more tolerant to a frequency shift in the experiments. Figure 8 shows the configuration of the bowtie slot antenna with corresponding dimensional parameters. The antenna is designed on the same substrate material as the harvester in Fig. 5. In the design, the two bowtie slot antenna elements are fed in phase and with the same amplitude by a Wilkinson power divider. Using two antenna elements, a higher antenna gain can be produced than a single element which can increase

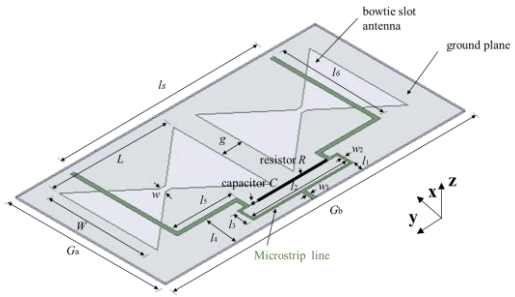

Fig. 8. The configuration of the bowtie slot antenna: L = 42 mm, W = 36 mm, g = 8 mm, l_s = 73.4 mm, l_1 = 5 mm, l_2 = 33 mm, l_3 = 6 mm, l_4 = 13.3 mm, l_5 = 21.7 mm, l_6 = 38 mm, w = 2 mm, w_1 = 1.29 mm, w_2 = 0.72 mm, G_a = 55 mm, and G_b = 110 mm.

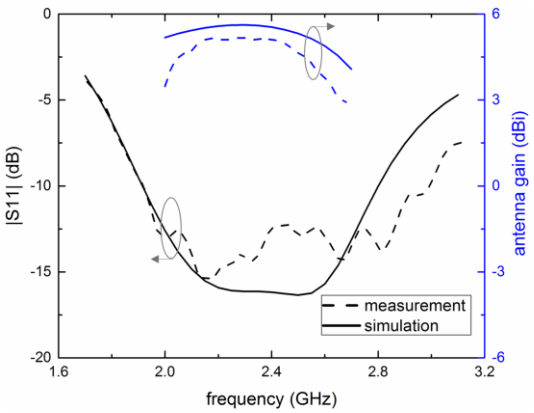

Fig. 9. Simulated and measured reflection coefficients and antenna gains of the bowtie slot antenna.

accessible RF power in the same power density environment [20-22].

Figure 9 shows the simulated and measured reflection coefficients of the antenna. As can be observed, a reasonable agreement can be obtained between the simulated and measured results. The measured impedance bandwidth is 43.9 % (1.92 GHz-3GHz), which is slightly larger than the simulated result of 37.3% (1.92 GHz-2.80 GHz) due to the unaccounted losses in the experiments. The impedance bandwidths of the antenna are wide enough for the narrow-band rectification.

The simulated and measured antenna gains at boresight direction (θ = 0° and ϕ = 0°) against frequency are also plotted in Fig. 9. Again, a reasonable consistency is observed. At 2.4 GHz, the simulated and measured antenna gains are 5.54 dBi and 5.07 dBi, respectively.

Figure 10 shows the measured and simulated radiation patterns of the antenna at two elevation planes of ϕ = 0° and 90° at 2.4 GHz. As can be observed, the measured and simulated results agree with each other. The antenna has a bidirectional pattern with the maximum radiation at θ = 0° and 180°. The radiation patterns are stable across the impedance bandwidth.

B. Rectenna

In order to test the rectenna under different RF source power levels, the received power against the distance between the transmitting antenna and proposed bowtie slot antenna is investigated first. Figure 11 shows the measurement setup. To exclude the interference from free space, the experiment is

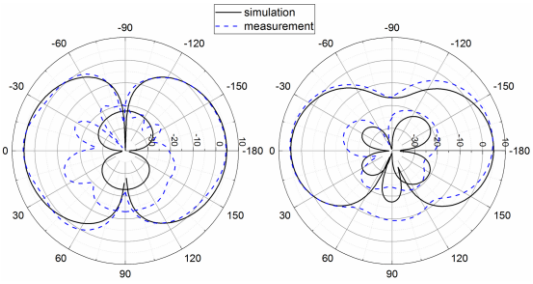

ϕ = 0° ϕ =90°

Fig. 10. Simulated and measured radiation patterns of bowtie slot antenna at elevation planes of ϕ = 0° and 90°.

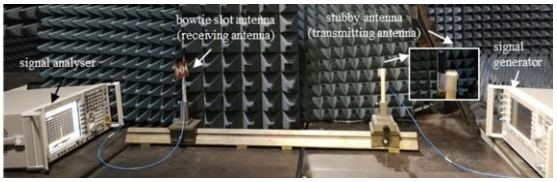

Fig. 11. Measurement setup for measuring received RF power using the bowtie slot antenna.

conducted in the anechoic chamber. In the experiment, a stubby antenna as transmitting antenna is connected to a signal generator with output power of 0 dBm, to mimic the low-power RF environment. The designed receiving bowtie slot antenna is connected to a signal analyzer for measuring the received RF power. Both the transmitting and receiving antennas are placed onto a triangular track for fixing and marking the position. The position of the transmitting antenna is defined as the original point. By moving away from the transmitting antenna, the receiving antenna is able to receive different RF power levels.

The transmitting power density P_d using Friis transmission equation [23] can be calculated by:

$$P_d = \frac{P_t G_t}{4\pi R^2} \tag{17}$$

where P_t and G_t are the power and antenna gain of the transmitting antenna, respectively. R is the distance between transmitting and receiving antenna. If the antenna gain of a receiving antenna is defined as G_r, the received power can be given by:

$$P_r = \frac{G_r \lambda^2}{4\pi} \frac{P_t G_t}{4\pi R^2} \tag{18}$$

In the experiments, the distance between the transmitting and receiving antenna R is varied in a range of 30 -80 cm, due to the limitation of the cable and track lengths. The distance range satisfies the far-field region condition of the transmitting antenna at 2.4 GHz ($R \geq$ 4 cm). Figure 12 shows the measured RF power as a function of distance R. The cable loss of receiving antenna is compensated here. According to Fig.12, when the receiving bowtie slot antenna is moved away from 30 to 80 cm, the received RF power level can be changed from −27 to −37 dBm. Using the plot in Fig. 12, the received power can be directly related to the distance.

The bowtie slot antenna is integrated with the proposed mixed cooperative power harvester, forming a rectenna. To avoid the matching loss between the antenna and harvester, the rectenna is developed by directly matching the antenna port to the input of the diode [24]. Figure 13 shows the prototype of the proposed rectenna. The load resistor (R_L) is kept as 5.6 kΩ that

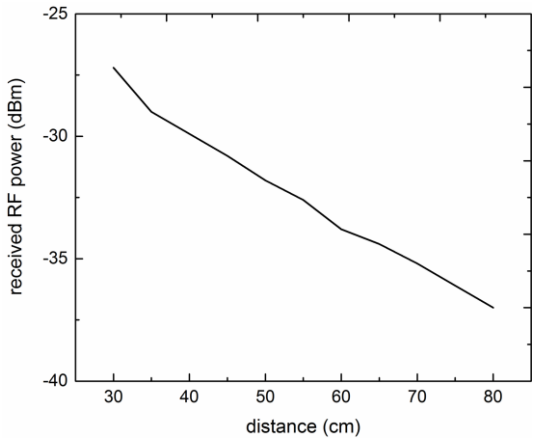

Fig. 12. Measured RF power received by bowtie slot antenna against distance away from the transmitting antenna.

(a) (b)

Fig. 13. The prototype of the proposed rectenna without matching network. (a) Ground plane layer showing the two etched bowtie slot elements. (b) Circuit layout showing antenna's feeding network and connected harvester without matching network.

is equal to the value in the previous power harvester. It should be mentioned that the theoretical analysis is still valid for this case, as the transmitting antenna can only provide the RF source around the design frequency of interest without involving the higher-order harmonics. Also, the direct conjugate matching between the antenna and harvester ports only works at the design frequency due to the impedance variation of the two ports.

Figure 14 shows the measurement setup for the proposed rectenna, using the same setup condition as shown in Fig. 11. For the output dc voltage of TEG, it still uses preliminarily determined values given in previous section which is monitored by a multi-meter as indicated in Fig. 14. To measure the output dc power, another multi-meter is deployed. Figure 15 shows the measured output dc power of rectenna with mixed power sources and that with a single RF source against the received RF power. The dc power converted by TEG is kept the same as the received RF power. When the received RF power is around −30 dBm, the output power of 0.754 μW and 0.067 μW are measured for the two aforementioned cases. The values are consistent with the results obtained in the previous harvester without the antenna, validating the rectenna design. As expected, higher output dc power is observed in the rectenna with mixed cooperative power sources. For comparison, the rectenna with L matching network is also fabricated and measured with the result given in Fig. 15.

It was found that the output dc power around 0.7 μW is obtained under the same input power condition (−30 dBm).

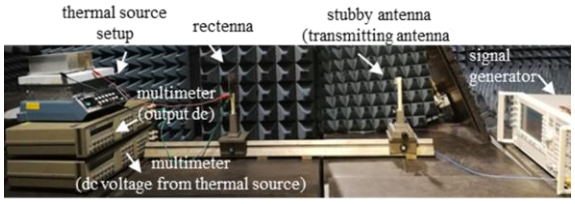

Fig. 14. Measurement setup of the proposed rectenna.

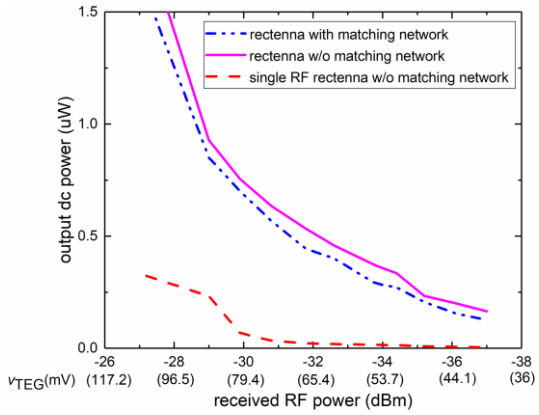

Fig. 15. Measured output dc power of the rectenna eliminating matching network with two power sources, the retenna eliminating matching network with only RF input, and the rectenna with L matching network against the measured RF power. The thermal source power is kept the same as the received RF power.

This is reasonable as the matching network will introduce insertion loss which reduces the power reaching the diode. The less injecting power into the diode results in lower RF-to-dc PCE and final total PCE. The matching network effects can be further investigated using a similar model shown in [25]. As the diode impedance changes slightly in the designed power level due to the parasitic capacitance, a simple L matching network is used in the design. Also, acceptable matching performance of the rectenna eliminating the matching network can be obtained over the measured power range because of a slight variation of the diode impedance. Referring to the curves in Fig. 15, the rectenna without the matching network can produce a higher output power than that with the simple *L* matching network. This is also reasonable as the former rectenna can eliminate the loss of matching network, if the matching conditions of both rectennas are acceptable.

Table II shows a comparison between the proposed mixed power harvester and previous designs. From the perspective of the energy availability, RF power can be continuously obtained unless in blackout situations. But considering the low power density of RF power, the output power of pure RF power harvesters is usually limited [26-28]. By incorporating several power sources, the hybrid/mixed harvester is not only a way of producing more power but also a reliable way of improving the resilience of the dc power production (given that the two energy sources are uncorrelated) [9,10],[12-15]. Although solar and artificial light sources have large power densities, they are limited by weather condition and human activities. A simple combination of the solar/light and RF sources can only improve the output power without increasing RF-to-dc PCE [9,12]. In [13], a seamless incorporation of solar, thermal and RF sources results in a high complexity of the device. For enhancing the total PCE, the cooperative kinetic and RF power harvester was developed, but it shows a relatively large size and relatively low output power due to a low power density [10,15]. The thermal power is also intermittent source and sometimes relies on a heat sink for maintaining the temperature gradient. It is employed as a bias of a diode with the RF-to-dc PCE leveraged [14]. However, the theoretical analysis of the diode conversion, the RF-to-dc enhancement, and the key controlling parameters were not clearly given. As shown in the Table II, the proposed topology shows the maximum RF-to-dc PCE at the ambient power level among these hybrid/mixed power harvesters. Besides, the accurate model takes the parasitic components of the diode into consideration and can accurately predict the diode's performance in the single or mixed power source injecting scenarios. Moreover, the proposed method reveals parameters controlling the RF-to-dc PCE, providing a clue for selecting a proper diode.

Figure 16 shows a realistic application scenario in an office building with Wi-Fi coverage. By placing the TEG on the window, the temperature gradient can be obtained by the temperature difference between indoor and outdoor. The indoor room temperature is generally stabilized at 20 °C all the year around, but the temperature outside varies and can be even down to − 40 °C in winter providing enough temperature gradient for power harvesting.

Table II Comparison of previous power harvesters

	Energy availability	Injecting energy	Input RF power level (dBm)	Meas. total PCE (@−30dBm)	Meas. RF-dc PCE (@−30dBm)	Device complexity [29]	Theoretical analysis
[26]	Continuous	High-freq.@ 2.45 GHz	−30 to 15	10%	10%	Simple	No
[27]	Continuous	High-freq.@0.9&1.8&2.1GHz	−40 to −10	15%	15%	Medium	No
[28]	Continuous	High-freq.@ 1.8-2.5 GHz	−35 to −10	10.7%	10.7%	Medium	No
[9]	Day time (S) Continuous (R)	DC(S) &High-freq. @ 0.85& 1.85 GHz	−25 to −10	N.A.	15%@−20dBm	Medium	No
[10] & [15]	Intermittent(K) Continuous (R)	Low-freq. AC (K) & High-freq.@1.8 GHz	−45 to −30	5.35%	N.A.	Medium	Yes
[12]	Intermittent (L) and (T)	DC(L) and (T)	N.A.	N.A.	N.A.	Medium	No
[13]	Intermittent (T) Day time (S) Continuous (R)	DC (T) &DC (S) & High-freq. @2.45 GHz	N.A.	N.A.	N.A.	High	No
This work	Intermittent (T) Continuous (R)	DC (T) & High-freq. @ 2.4 GHz	−45 to −25	40%@−30dBm 32%@−40dBm	33.4%@−30dBm 14.3%@−40dBm	Medium	Yes

(T) Thermal energy, (R) RF energy, (S) solar energy, (K) kinetic energy.

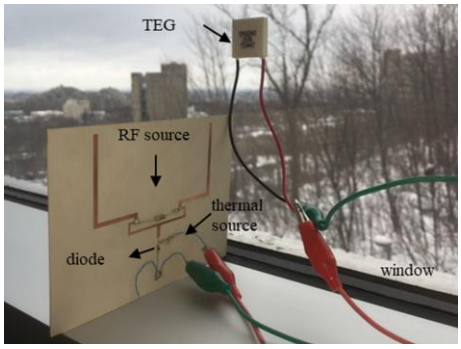

Fig. 16. An application scenario of interest.

V. Conclusion

In this paper, a mixed cooperative ambient power harvester scavenging RF and thermal energy for low-power application scenarios has been designed, rigorously analyzed, simulated and measured. The harvested dc power from thermal source is deployed for biasing the diode, in order to improve RF-to-dc PCE. To predict the diode's performance in this scenario, an accurate model was proposed. Using the model, RF-to-dc PCE relevant parameters are specified. This model can be useful as a rough guideline for selecting a proper diode in such a mixed power harvester. The model takes the parasitic components of the diode and the load resistor into consideration, thus showing a more realistic model. Precise prediction of output dc power and RF-to-dc PCE can be given for Schottky diode in such a mixed cooperative power input condition. In the design example, a typical diode model of SMS7630 is used for validating the analytical formulation.The evaluation of the diode is shown with each related parameter affecting the resultant RF-to-dc PCE. The calculated RF-to-dc PCE was verified by the simulated one. The prototype of the mixed cooperative power harvester was fabricated for further validation. It was found that the measured dc power reasonably agrees with the calculated and simulated results in the power range of interest.

Besides, a systemic rectenna design including the antenna design and RF environment setup is clear given. The proposed rectenna integrating a bowtie slot antenna was designed with the antenna port matched to the diode directly. It is measured under different RF power conditions. The dc power harvested from thermal source is kept the same as RF source. When the two power sources are both around −30 dBm, the output power of 0.754 μW is obtained. Besides, the output dc power is higher than the counterpart in the rectenna using simple *L* matching network.

The proposed mixed power harvester is capable of leveraging the RF-to-dc PCE, thereby showing its usefulness in a situation considering economical relevant issues.

Acknowledgement

The authors would like to express gratitude to the technical support team of Poly-Grames Research Center, who are J. Gauthier, D. Dousset and T. Antonescu.

References

[1] K. Rose, S. Eldridge, and L. Chapin, "The internet of things: An overview," *The Internet Society (ISOC)*, pp. 1-50, Oct. 2015

[2] S. Kim, R. Vyas, J. Bito, K. Niotaki, A. Collado, A. Georgiadis, *et al.*, "Ambient RF energy-harvesting technologies for self-sustainable standalone wireless sensor platforms," *Proceedings of the IEEE*, vol. 102, no. 11, pp. 1649-1666, Nov. 2014

[3] A. S. Weddell, *et al.*, "A survey of multi-source energy harvesting systems," in *2013 Design, Automation& Test in Europe Conference & Exhibition (DATE)*, pp. 905-908,Mar. 18-22, 2013,.

[4] A. Khaligh, P. Zeng, C. Zheng, "Kinetic energy harvesting using piezoelectric and electromagnetic technologies – state of the art", *IEEE Trans. Ind. Electron.*, vol. 57, no. 3, pp. 850-860, Mar. 2010.

[5] Z. Zhang, H.L.Pang, A.Georgiadis, and C. Cecati,"Wireless power transfer-an overview," *IEEE Trans. Ind. Electron.*, vol. 66, no. 2, pp. 1044-1058, May 2018.

[6] S. Hemour *et al.*, "Towards low-power high-efficiency RF and microwave energy harvesting," *IEEE Trans. Microw. Theory Tech.*, vol. 62, no. 4, pp. 965–976, Apr. 2014

[7] C. H. P. Lorenz, S. Hemour, W. Li, Y. Xie, J. Gauthier, P. Fay, et al., "Breaking the Efficiency Barrier for Ambient Microwave Power Harvesting With Heterojunction Backward Tunnel Diodes," *IEEE Trans. Microw. Theory Tech*, vol. 63, no. 12 pp. 4544-4555, Dec. 2015.

[8] A. Sharma, V. Singh, T. L. Bougher, and B. A. Cola, "A carbon nanotube optical rectenna," *Nature nanotechnology*, vol.10, pp. 1027-1032, Sep.2015.

[9] A. Collado and A. Georgiadis, "Conformal hybrid solar and electromagnetic (EM) energy harvesting rectenna," *IEEE Trans. Circuits Syst. I, Reg. Papers*, vol. 60, no. 8, pp. 2225–2234, Aug. 2013

[10] C. H. Lorenz, *et al.*, "Hybrid power harvesting for increased power conversion efficiency," *IEEE Microw.Wireless Compon. Lett.*, vol. 25, no. 10, pp. 687-689, Oct. 2015..

[11] V. Leonov, "Thermoelectric energy harvesting of human body heat for wearable sensors," *IEEE Sensors J.*, vol. 13, no. 6, pp. 2284–2291, Jun. 2013.

[12] Y. K. Tan and S. K. Panda, "Energy harvesting from hybrid indoor ambient light and thermal energy sources for enhanced performance of wireless sensor nodes," *IEEE Trans. Ind. Electron.*, vol. 58, no. 9, pp. 4424–4435, Sep. 2011

[13] S. Lemey, F. Declercq, and H. Rogier, "Textile antennas as hybrid energy harvesting platforms," *Proceedings of the IEEE*, vol. 102, no. 11, pp. 1833-1857, Oct. 2014

[14] M. Virili *et al.*, "Performance improvement of rectifiers for WPT exploiting thermal energy harvesting," *Wireless Power Transfer*, vol. 2, no. 1, pp. 22-31, Apr. 2015.

[15] X. Q. Gu, W. Q. Liu, L. Guo, S. Hemour. F. Formosa, A. Badel, and K. Wu, "Hybridization of integrated microwave and mechanical power harvester " *IEEE Access*, vol. 6, pp 13921-13930, Mar. 2018.

[16] G. Mahan, B. Sales, and J. Sharp, "Thermoelectric materials: New approaches to an old problem," *Phys. Today*, vol. 50, no. 3, pp. 42–47, Mar. 1997

[17] F. Bolos, *et al.*, "RF Energy Harvesting From Multi-Tone and Digitally Modulated Signals," *IEEE Trans. Microw. Theory Techn.*, vol. 64, no. 6, pp. 1918-1927, Jun. 2016

[18] X. Gu, L. Guo, S. Hemour, and K. Wu, "Accurate Analytical Model for Hybrid Ambient Thermal and RF Energy Harvester," in *IEEE MTT-S Int. Microw. Symp. Dig.*, pp 1-3, Jun. 2018.

[19] C. H. P. Lorenz, S. Hemour, and K. Wu, "Physical mechanism and theoretical foundation of ambient RF power harvesting using zero-bias diodes," *IEEE Trans. Microw. Theory Tech*, vol. 64, no. 7, pp. 2146-2158, Jul. 2016.

[20] H. Sun, Y. X. Guo, M. He, and Z. Zhong, "Design of a high-efficiency 2.45-GHz rectenna for low-input-power energy harvesting," *IEEE Antennas Wireless Propag. Lett.*, vol. 11, pp. 929–932, Aug. 2012

[21] C. H. Chin, Q. Xue, and C. H. Chan, "Design of a 5.8-GHz rectenna incorporating a new patch antenna," *IEEE Antennas Wireless Propag. Lett.*, vol. 4, pp. 175–178, Jun. 2005.

[22] E. Vandelle *et al.*, "High gain isotropic rectenna," in *IEEE Wireless Power Transfer Conference*, May 10-12, 2017.

[23] J. D. Kraus and R. J. Marhefka, Antennas for all applications, 3rd ed., McGraw Hill, New York, 2003.

[24] C. Y. Song, Y. Huang, J. F. Zhou, P. Carter, S. Yuan, Q. Xu, and Z X. Fei, "Matching network elimination in broadband rectennas for

high-efficiency wireless power transfer and energy harvesting," *IEEE Trans. Ind. Electron.*, vol. 64. no. 5, pp. 3950-3961, May. 2017.
[25] A. M. Niknejad, Electromagnetics for high-speed analog and digital communication circuits, Cambridge University Press, 2007.
[26] H. Sun, Y.-X. Guo, M. He, and Z. Zhong, "Design of a highefficiency 2.45-GHz rectenna for low-input-power energy harvesting," *IEEE Antennas Wireless Propag. Lett.*, vol. 11, pp. 929–932, Aug. 2012.
[27] S. P. Shen, C. Y. Chiu, R. D. Murch, "A dual-port triple-band L-probe microstrip patch rectenna for ambient RF energy harvesting," *IEEE Antennas Wireless Propag. Lett.*, vol. 16, pp. 3071–3074, Oct. 2017.
[28] C. Song, Y. Huang, J. Zhou, J. Zhang, S. Yuan, and P. Carter, "A high efficiency broadband rectenna for ambient wireless energy harvesting," *IEEE Trans. Antennas Propag.*, vol. 63, no. 8, pp. 3486–3495, Aug. 2015.
[29] O. B. Akan, O. Cetinkaya, C. Koca, and M. Ozger, "Internet of hybrid energy harvesting things," *IEEE Internet of Things Journal*, vol. 5, no. 2, pp. 736-746, Apr. 2018.

Lei Guo received the B.Eng. degree in communication engineering from the Harbin Institute of Technology, Harbin, China, in 2011, and the Ph.D. degree in electronic engineering from the City University of Hong Kong, Hong Kong, China, in 2016. From 2016 to 2019, she was a postdoctoral research fellow with Poly-Grames Research Center, Polytechnique Montreal, Canada. She is currently an Associate Professor with the School of Information and Communication Engineering, Dalian University of Technology, Dalian, China. She received the 2015 iWEM Student Best Paper Award. She served as the organizing committee member and Chair of student best design and paper competition of 2018 IEEE IEEE MTT-S Wireless Power Transfer Conference, Montreal, QC, Canada. Her current research interests include dielectric resonator antenna, antenna in package, and energy harvesting.

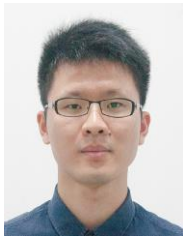

Xiaoqiang Gu (GS'17) was born in Changzhou, China, in 1990. He received the B.Eng. degree from the University of Electronic Science and Technology of China, Chengdu, China, in 2012, and the M.Eng. degree from Zhejiang University, Hangzhou, China, in 2015. He is currently pursuing the Ph.D. degree at the École Polytechnique de Montréal, Montréal, QC, Canada. His current research interests include wireless power harvesting, multi-source energy harvesting, and nonlinear circuit analysis and design.
Mr. Gu was a recipient of the 2019 IEEE MTT-S Graduate Fellowship Award, the Best Student Paper Award at 2017 IEEE MTT-S Wireless Power Transfer Conference, Taipei, Taiwan, R.O.C., and the Travel Grant Award at 2018 IEEE MTT-S International Microwave Workshop Series on 5G Hardware and System Technologies, Dublin, Ireland. He was also among the Best Student Paper Finalists at 2018 IEEE MTT-S Wireless Power Transfer Conference, Montreal, QC, Canada.

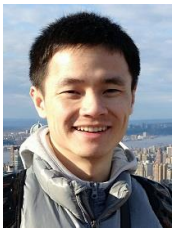

Peng Chu (S'10–M'14) was born in Anqing, China, in 1985. He received the B.S. and M.S. degrees from Xidian University, Xi'an, China, in 2006 and 2009, respectively, and the Ph.D. degree from the State Key Laboratory of Millimeter Waves, Southeast University, Nanjing, China, in 2014. Since 2014, he has been a Lecturer with the College of Electronic and Optical Engineering, Nanjing University of Posts and Telecommunications, Nanjing. Since 2018, he has been a Postdoctoral Fellow with the Ecole Polytechnique de Montréal, University of Montreal, Montréal, QC, Canada. His current research interests include microwave and millimeter-wave circuits and antennas and energy harvesting.

Simon Hemour (S'08–M'11–SM'16) received the B.S. degree in electrical engineering from the University of Grenoble, Grenoble, France, in 2004, and the M.S. and Ph.D. degrees in optics, optoelectronics, and microwave engineering from the Grenoble Institute of Technology, Grenoble, France, in 2006 and 2010, respectively.
From 2006 to 2007, he was a Research Assistant with the Pidstryhach Institute of Applied Problems of Mechanics and Mathematics, National Academy of Science of Ukraine, Lviv, Ukraine. In 2003, he joined the European Organization for Nuclear Research, Geneva, Switzerland, as a member of the Instrumentation Department, where he was involved with ATLAS experiment on the large Hadron collider. In 2007, he joined the IMEP-LAHC MINATEC Laboratory, Grenoble, France. From 2011 to 2015, he was with the Poly-Grames Research Center, Ecole Polytechnique de Montreal, Montreal, QC, Canada, where he was leading the Wireless Power Transmission and Harvesting Research Group. He joined the Universite de Bordeaux, Bordeaux, France, in 2015, where he is currently an Associate Professor, and he leads research in wireless micro energy solutions for IoT and biomedical applications. His current research interests include wireless power transfer and hybrid energy harvesting, nonlinear devices, innovative RF measurements, RF interferometry, low power microwave, and millimeter-wave conversion circuits.
Dr. Hemour is a member of the IEEE MTT-26 Wireless Energy Transfer and Conversion Technical Committee.

Ke Wu (M'87–SM'92–F'01) received the B.Sc. degree (Hons.) in radio engineering from Southeast University, Nanjing, China, in 1982, the D.E.A. degree (Hons.) in optics, optoelectronics, and microwave engineering from the Institut National Polytechnique de Grenoble, Grenoble, France, in 1984, and the Ph.D. degree (Hons.) in optics, optoelectronics, and microwave engineering from the University of Grenoble, Grenoble, France, in 1987.
He was the Founding Director of the Center for Radiofrequency Electronics Research of Quebec (Regroupement Stratgique of FRQNT). He has held guest, visiting, and honorary professorships with many universities around the world. He is currently a Professor of electrical engineering, the Tier-I Canada Research Chair in RF and millimeter-wave engineering, and the NSERC-Huawei Industrial Research Chair in future wireless technologies with the Ecole Polytechnique de Montreal, Montreal, QC, Canada, where he has been the Director of the Poly-Grames Research Center. He has authored or co-authored over 1000 refereed papers and a number of books/book chapters. He holds over 30 patents. His current research interests include substrate integrated circuits, antenna arrays, advanced computer aided design and modeling techniques, nonlinear wireless technologies, wireless power transmission and harvesting, development of RF and millimeter-wave transceivers and sensors for wireless systems and biomedical applications, and the modeling and design of microwave and terahertz photonic circuits and systems.
Dr. Wu is a fellow of the Canadian Academy of Engineering and the Royal Society of Canada (The Canadian Academy of the Sciences and Humanities). He is a member of Electromagnetics Academy, Sigma Xi, and URSI. He was a recipient of many awards and prizes, including the first IEEE Microwave Theory and Techniques (IEEE MTT-S) Outstanding Young Engineer Award, the 2004 Fessenden Medal of the IEEE Canada, the 2009 Thomas W. Eadie Medal of the Royal Society of Canada, the Queen Elizabeth II Diamond Jubilee Medal in 2013, the 2013 FCCP Education Foundation Award of Merit, the 2014 IEEE MTT-S Microwave Application Award, the 2014 Marie-Victorin Prize (Prix du Quebec the highest distinction of Quebec in the natural sciences and engineering), the 2015 Prix dExcellence en Recherche et Innovation of Polytechnique Montreal, and the 2015 IEEE Montreal Section Gold Medal of Achievement. He was an IEEE MTT-S Distinguished Microwave Lecturer from 2009 to 2011. He is the IEEE MTT-S President. He is the Inaugural Three-Year Representative of North America as a Member of the European Microwave Association General Assembly. He was an Elected IEEE MTT-S Administrative Committee (AdCom) Member from 2006 to 2015. He has served as the Chair of the IEEE MTT-S Transnational Committee, the IEEE Member and Geographic Activities Committee, and the Technical Coordinating Committee among many other AdCom functions. He has held key positions in and has served on various panels and international committees, including the Chair of Technical Program Committees, International Steering Committees, and international conferences/symposia. In particular, he was the General Chair of the 2012 IEEE MTT-S International Microwave Symposium. He was the Chair of the joint IEEE Chapters of MTT-S/AP-S/LEOS, Montreal, QC, Canada. He is the Chair of the newly restructured IEEE MTT-S Montreal Chapter. He has served on the Editorial/ Review Boards of many technical journals, transactions, proceedings, and letters, and also scientific encyclopedia, including as an Editor or a Guest Editor.